

---

# Time-Resolved Optical Response of All-Oxide, $\text{YBa}_2\text{Cu}_3\text{O}_7/\text{La}_{0.7}\text{Sr}_{0.3}\text{MnO}_3$ Proximitized Bilayers

The interplay between superconductivity (S) and ferromagnetism (F) is one of the most intriguing and challenging fields of research in solid-state physics. The proximity effect at the interface between traditional, both metallic, S and F films has been widely investigated.<sup>1</sup> In comparison, properties of bilayers consisting of high-temperature superconducting cuprates and ferromagnetic manganites are much less understood, despite large research activities and substantial progress in the comprehension of the physics of the involved materials.<sup>2–4</sup> The superconducting proximity effect at the S/F interface is governed by the short coherence length of the cuprate  $\xi_0 \approx v_F/2\Delta$  and by the even shorter coherence length  $\xi_m \approx v'_F/2E_b$  in manganites, where  $v_F$  and  $v'_F$  are the Fermi velocities in the S and F layers, respectively,  $\Delta$  is the superconducting energy gap, and  $E_b \approx 3$  eV is the manganite exchange energy.<sup>5</sup> At the interface, a layer with a thickness of about  $\xi_0$  within the superconductor is expected to show a depressed superconductivity that, in combination with extremely short  $\xi_m$ , suggests that Cooper pairs should not practically penetrate into the F layer. This simple consideration is, however, still subject to debate since an unexpected long-range proximity effect recently reported<sup>3,6,7</sup> has been ascribed to the spin superconducting triplet-pairing at the F side of the bilayer in the presence of magnetic inhomogeneities or domain walls.<sup>6,8</sup> Magnetic properties of the S/F interface, on the other hand, are governed by the short-length exchange field and associated to nonconventional ordering of Cu spins,<sup>4</sup> while longer-range effects depend on the spin-diffusion mechanism.<sup>9</sup> Finally, the establishment of the equilibrium chemical potential determines a charge transfer,<sup>2</sup> with screening length of the order of 1 to 2 nm, determining “dead layers” on both the S and F sides.

Cuprate/manganite oxide, nanostructured heterostructures are likely to have a high potential for applications. Beside a constantly growing field of spintronics, our research attention has been devoted to  $\text{YBa}_2\text{Cu}_3\text{O}_7/\text{La}_{0.7}\text{Sr}_{0.3}\text{MnO}_3$  (YBCO/LSMO) hybrids as possible, artificially engineered, ultrafast optoelectronics devices.<sup>10,11</sup> However, nonequilibrium properties of the S/F bilayers are far from being fully characterized

and understood. Time-resolved pump–probe ultrafast optical spectroscopy can provide a great deal of information on the dynamics of such complex structures.<sup>12</sup> In this article, we present the successful fabrication of epitaxial YBCO/LSMO nanobilayers and their subpicosecond pump–probe characterization in a temperature range below and above the superconducting critical temperature  $T_c$ .

Our YBCO/LSMO heterostructures were grown by pulsed-laser deposition on (001)  $\text{SrTiO}_3$  substrates (with a single  $\text{TiO}_2$  termination layer), in an  $\text{O}_2$  atmosphere at 0.25-Mbar pressure, for deposition of both the first (YBCO) and the second (LSMO) layers. The growth process was performed at 800°C and was controlled *in situ* by the reflection high-energy electron diffraction (RHEED) method. The RHEED patterns demonstrated very high crystallinity of our bilayer structures at every step of the process.<sup>10</sup> Cooling of the samples included a prolonged exposure to 200 Mbar of  $\text{O}_2$  at 500°C, to promote full oxidation of YBCO through the LSMO capping. The resulting nanostructures had excellent structural and transport properties, with  $\sim 0.3^\circ$  full-width-at-half-maximum rocking curves and sharp superconducting transition ( $T_{c0}$  up to 91.5 K,  $\Delta T_c \sim 0.3$  K). From measurements of the conductivity's dependence on temperature, we could deduce that the Curie temperature  $T_c$  of LSMO largely exceeded room temperature, concluding that in our experiments, even under optical illumination, the LSMO film always remained in the ferromagnetic state. Our test samples consisted of a plain, 100-nm-thick YBCO film (a reference sample) and a sequence of 100-nm-thick YBCO layers capped with 10 and 35 nm of LSMO, respectively (named LY10 and LY35, respectively). The LSMO thicknesses guaranteed a partially transparent behavior at near-infrared wavelengths since, based on our conductivity data, the optical penetration depth was estimated to be

$$\delta \approx \sqrt{\frac{2\varepsilon_0 c^2}{\sigma_0 \omega}} \approx 100 \text{ nm}$$

at our lowest test temperatures.

The femtosecond pump–probe spectroscopy experiments were performed using a mode-locked Ti:sapphire laser, which produced 100-fs pulses at 810-nm wavelength and a 76-MHz repetition rate. The pump and probe beams were focused onto the sample, down to 30  $\mu\text{m}$  in diameter, and cross polarized to eliminate the coherent artifact caused by the direct interference of the two beams. The pump-to-probe average power ratio was set at 10:1 with the pump power set at the 30-mW level (400 pJ of energy per pulse), in order to minimize optical heating and, simultaneously, ensure a good signal-to-noise ratio. The samples were mounted on a cold finger, inside a temperature-controlled, liquid-helium, continuous-flow optical cryostat, operating down to 4 K.

Typical recorded data of the relative optical-reflectivity change  $\Delta R/R$  versus time delay are presented in Fig. 127.26. Figure 127.26(a) shows the  $\Delta R/R(t)$  waveforms for the reference 100-nm-thick YBCO film, recorded at different temperatures.

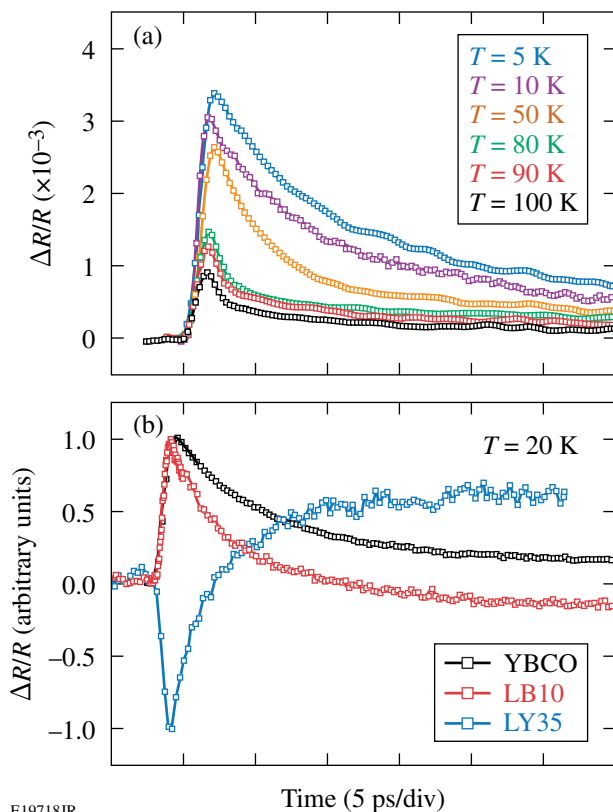
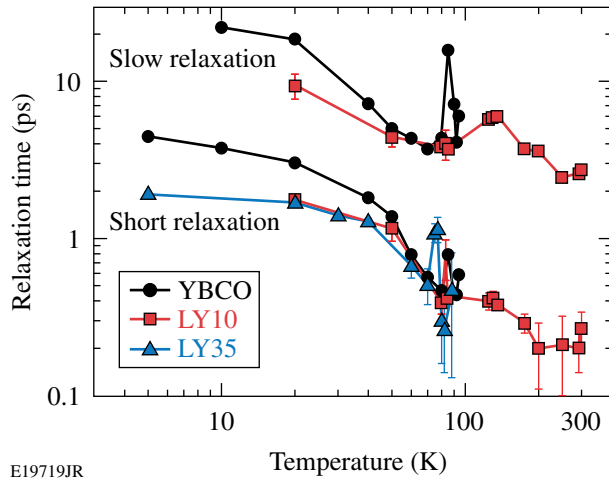


Figure 127.26 (a) The photoresponse  $\Delta R/R$  transient versus delay time for a 100-nm-thick YBCO film at different temperatures. (b) The normalized  $\Delta R/R$  waveforms versus delay time measured at 20 K for the reference YBCO film and the LY10 and LY35 S/F bilayers.

According to earlier studies on high- $T_c$  materials,<sup>13</sup> the amplitude of the  $\Delta R/R$  signal grows below  $T_c$ , while, simultaneously, the recovery becomes progressively slower. This is consistent with other pump–probe studies performed under low-fluence excitations.<sup>13,14</sup> Contrary to some earlier observations,<sup>15,16</sup> our data are fitted by a simple linear recombination model, and weak, damped oscillations on top of the exponential decay might, tentatively, be ascribed to displaced excitation of coherent acoustic phonons.<sup>15,17</sup> Overall, our observations for the pure YBCO film are in agreement with reported data<sup>14,18–20</sup> and corroborate current interpretation that the slow dynamics below  $T_c$  (several tens of picoseconds) cannot be ascribed to the acoustic phonon bottleneck, in contrast with the case of low- $T_c$  superconductors.<sup>21</sup> In high- $T_c$  materials, recombination of two quasiparticles into a Cooper pair by emission of an acoustic phonon is, in fact, forbidden because the quasiparticle's velocity is faster than the sound velocity<sup>22</sup> and the Cooper-pair recombination reflects a complex kinematics involving both nodal and anti-nodal quasiparticles.<sup>18,19</sup>

The  $\Delta R/R$  transients collected at 20 K for two YBCO/LSMO bilayers (LY10 and LY35) and the YBCO reference sample are shown in Fig. 127.26(b). We observe that the thickness of the LSMO overlayer is critically important to the bilayer photoresponse. While the functional dependence of waveform LY10 follows that of the YBCO sample, although with reduced relaxation time, the LY35 curve is very different: it consists of a negative initial peak, followed by an extended relaxation tail, which crosses into the positive values of the  $\Delta R/R$  dependence. The negative peak with a time constant  $\leq 1$  ps can be due to the presence of an additional relaxation mechanism related most likely to localized traps at the S/F interface<sup>23</sup> or multiple reflection from thin heterostructures.

During the course of our research, we have collected dozens of  $\Delta R/R$  waveforms for all three samples in the temperature range from 4 K to 300 K, under nominally the same optical pump–probe conditions, and have fitted the data with bi-exponential functions containing two characteristic relaxation times. The latter was justified by the assumption that well above  $T_c$ , the system is simply governed by subpicosecond-in-duration, hot-electron cooling in our two materials, of which LSMO has a somewhat slower relaxation time, while below  $T_c$ , the fast relaxation process is related to the electron–phonon interaction and the slow one corresponds to the quasi-particle recombination. The results are summarized in Fig. 127.27, where we plot the fast and slow relaxation time dependences on temperature. First we note that below  $T_c$ , our YBCO/LSMO bilayers have relaxation times shorter than YBCO, in agreement with the



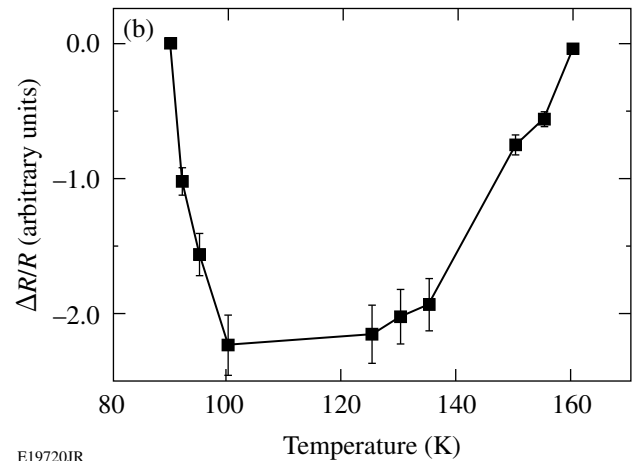
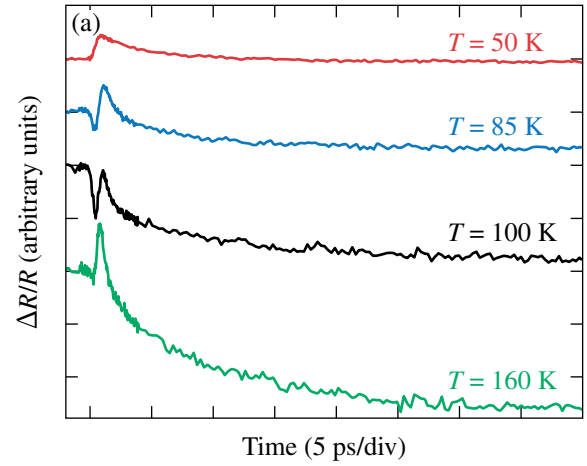
E19719JR

Figure 127.27

The characteristic, both short and slow, relaxation times extracted from the  $\Delta R/R(t)$  plots for all our tested samples as a function of temperature.

YBCO/Au/NiCu case.<sup>10</sup> We also observe the presence of sharp peaks in both the fast and slow (YBCO only) relaxation time dependences, which we believe correspond to the occurrence of a superconducting transition within the probed samples, reflecting the change in the quasi-particle dynamics caused by the electronic-specific heat jump.<sup>21,24</sup> As expected, the  $T_c$  peak feature shifts slightly to lower temperatures for the thicker LSMO overlayers but, most interestingly, still remains well visible, contrary to metallic, S/F proximitized bilayers.<sup>25</sup> Finally, we note that the characteristic time constant of heat transfer from phonons to the spin-wave gas in LSMO below  $T_c$  (Ref. 26) is of the order of 30 ps; consequently, it is essentially out of scale in our measurements.

The active role of the S/F interface results in a clear difference between the dynamics of the bilayers and the mere superposition of behaviors of components films. This is well illustrated by LY10 data shown in Fig. 127.28. Figure 127.28(a) presents examples of the  $\Delta R/R$  curves well below  $T_c$ , in the vicinity of  $T_c$ , and, finally, high above  $T_c$ . As mentioned above, in a range of temperature above  $T_c$ , we observe a sharp undershoot that precedes the positive  $\Delta R/R$  peak. As demonstrated in Fig. 127.28(b), the undershoot quickly increases its magnitude at the superconducting transition, reaching the maximum value at  $\sim 100$  K, remains roughly constant negative in the  $\sim 100$ -K to 140-K range, and finally disappears at  $\sim 160$  K. We stress that no undershoot has ever been observed in either pure LSMO or YBCO films. In our opinion, the undershoot reflects the presence of a few-nm-thick “dead layer” at the S/F interface, with degraded properties. This layer is a result of a charge



E19720JR

Figure 127.28

(a) Examples of photoresponse  $\Delta R/R$  transients versus delay time for an LY10 sample at different temperatures. The waveforms are shifted in the y axis for clarity. (b) The magnitude of the  $\Delta R/R$  negative peak (undershoot) versus temperature.

transfer from YBCO to LSMO that forms an underdoped YBCO region. The underdoped YBCO (e.g., an oxygen-poor compound) is well known to exhibit a sharp, negative  $\Delta R/R$  transient.<sup>27,28</sup> A similar behavior was also observed for underdoped  $\text{Bi}_2\text{Sr}_2\text{CaCu}_2\text{O}_{8+y}$  single crystals.<sup>29</sup>

The presence of both the depressed-superconductivity layer on the YBCO side and the degraded-magnetic layer on the LSMO side leads to another physical consideration. The quasi particles that are excited in bulk YBCO reach the interface in a characteristic time  $d/v_F \approx 100$  fs, comparable with our optical excitation pulse. The quasi-particle injection into the LSMO layer is inhibited because a half metal cannot host free electrons with both spin orientations. Reciprocally, hot electrons from LSMO cannot directly enter the YBCO layer

because they possess only one spin orientation. Within the underdoped YBCO, however, the quasi particles experience a much faster recombination in Cooper pairs since this region acts as an energy trap (suppressed  $\Delta$  region) that substantially shortens their relaxation process. The concept of excitations being trapped at the boundary between a superconductor and a half metal seems to be quite general and the subject certainly deserves further investigation, both experimental and theoretical. Our early results indicate, however, that this mechanism may efficiently enhance the speed of relaxation of an optically perturbed, nonequilibrium, high- $T_c$  superconductor, capped by the ultrathin F layer.

In conclusion, we investigated the temperature dependence of the nonequilibrium dynamics of YBCO/LSMO nanostructured bilayers in the temperature range from 4 K to room temperature. Experiments have demonstrated the active role of the S/F interface, where the electronic charge transfer from  $\text{La}_{0.7}\text{Sr}_{0.3}\text{MnO}_3$  to  $\text{YBa}_2\text{Cu}_3\text{O}_7$  determines a thin layer with degraded properties. The LSMO/YBCO bilayers are characterized by quasi-particle relaxation times that are shorter than those of the pure YBCO film, opening a new route to their possible applications in the field of ultrafast superconducting optoelectronics.

#### ACKNOWLEDGMENT

The authors gratefully acknowledge M. Cuoco for fruitful discussion and D. Pan for assistance in early experiments. The work was partially supported by the European Union under the MAMA project (Napoli, Italy) and by the NSF ECCS under Grant No. 0824075 (University of Rochester, Rochester, NY, USA).

#### REFERENCES

1. E. A. Demler, G. B. Arnold, and M. R. Beasley, *Phys. Rev. B* **55**, 15174 (1997).
2. S. Yunoki *et al.*, *Phys. Rev. B* **76**, 064532 (2007).
3. V. Peña *et al.*, *Phys. Rev. B* **69**, 224502 (2004).
4. J. Chakhalian *et al.*, *Nat. Phys.* **2**, 244 (2006).
5. J. Y. T. Wei *et al.*, *J. Appl. Phys.* **83**, 7366 (1998).
6. I. Asulin *et al.*, *Phys. Rev. B* **74**, 092501 (2006).
7. T. Holden *et al.*, *Phys. Rev. B* **69**, 064505 (2004).
8. A. F. Volkov, F. S. Bergeret, and K. B. Efetov, *Phys. Rev. Lett.* **90**, 117006 (2003).
9. S. Soltan, J. Albrecht, and H.-U. Habermeier, *Phys. Rev. B* **70**, 144517 (2004).
10. G. P. Pepe, L. Parlato, N. Marrocco, V. Pagliarulo, G. Peluso, A. Barone, F. Tafuri, U. Scotti di Uccio, F. Miletto, M. Radovic, D. Pan, and R. Sobolewski, *Cryogenics* **49**, 660 (2009).
11. N. Marrocco, G. P. Pepe, A. Capretti, L. Parlato, V. Pagliarulo, G. Peluso, A. Barone, R. Cristiano, M. Ejrnaes, A. Casaburi, N. Kashiwazaki, T. Taino, H. Myoren, and R. Sobolewski, *Appl. Phys. Lett.* **97**, 092504 (2010).
12. X. Zou *et al.*, *Appl. Phys. Lett.* **97**, 141910 (2010).
13. M. L. Schneider, S. Rast, M. Onellion, J. Demsar, A. J. Taylor, Y. Glinka, N. H. Tolks, Y. H. Ren, G. Lüpke, A. Xu, Y. Klimov, R. Sobolewski, W. Si, X. H. Zeng, A. Soukiassian, X. X. Xi, M. Abrecht, D. Ariosa, D. Pavuna, A. Krapf, R. Manzke, J. O. Printz, M. S. Williamsen, K. E. Downum, P. Guptaarma, and I. Bozovic, *Eur. Phys. J. B* **36**, 327 (2003).
14. N. Gedik *et al.*, *Science* **300**, 1410 (2003).
15. B. Mansart *et al.*, *J. Mod. Opt.* **57**, 959 (2010).
16. X. Li, Y. Xu, Š. Chromik, V. Štrbík, P. Odier, D. De Barros, and R. Sobolewski, *IEEE Trans. Appl. Supercond.* **15**, 622 (2005).
17. I. Bozovic, M. Schneider, Y. Xu, R. Sobolewski, Y. H. Ren, G. Lüpke, J. Demsar, A. J. Taylor, and M. Onellin, *Phys. Rev. B* **69**, 132503 (2004).
18. P. C. Howell, A. Rosch, and P. J. Hirschfeld, *Phys. Rev. Lett.* **92**, 037003 (2004).
19. C. W. Luo *et al.*, *J. Appl. Phys.* **102**, 033909 (2007).
20. X. Deng *et al.*, *Phys. Rev. B* **77**, 144528 (2008).
21. A. Rothwarf and B. N. Taylor, *Phys. Rev. Lett.* **19**, 27 (1967).
22. B. J. Feenstra *et al.*, *Phys. Rev. Lett.* **79**, 4890 (1997).
23. L. Vasiliu-Doloc *et al.*, *Phys. Rev. Lett.* **83**, 4393 (1999).
24. J. Demsar *et al.*, *Phys. Rev. Lett.* **82**, 4918 (1999).
25. T. Taneda, G. P. Pepe, L. Parlato, A. A. Golubov, and R. Sobolewski, *Phys. Rev. B* **75**, 174507 (2007).
26. R. D. Averitt and A. J. Taylor, *J. Phys. (USSR)* **14**, R1357 (2002).
27. L. Shi, T. Gong, X. Weng, Y. Kostoulas, R. Sobolewski, and P. M. Fauchet, *Appl. Phys. Lett.* **64**, 1150 (1994).
28. K. H. Wu *et al.*, *Chin. J. Phys.* **38**, 279 (2000).
29. Y. H. Liu *et al.*, *Phys. Rev. Lett.* **101**, 137003 (2008).